Contribution from the Department of Chemistry,
University of Wisconsin, Madison, Madison, Wisconsin 53706

# Stereochemical Analysis of $Fe_2(CO)_6(\mu\text{-}Se_2)$: A Diselenium Analogue of $Fe_2(CO)_6(\mu\text{-}S_2)$[1]

CHARLES F. CAMPANA,[2] FREDERICK YIP-KWAI LO, and LAWRENCE F. DAHL*[3]

*Received November 9, 1978*

The structure of $Fe_2(CO)_6(\mu\text{-}Se_2)$ has been determined by X-ray diffraction. The compound is isomorphous with triclinic $Fe_2(CO)_6(\mu\text{-}S_2)$ and crystallizes with two dimeric molecules in an unit cell of $P\bar{1}$ symmetry and of reduced cell parameters (at −95 ± 5 °C) of $a$ = 7.704 (2) Å, $b$ = 11.779 (6) Å, $c$ = 6.585 (3) Å, $\alpha$ = 104.86 (4)°, $\beta$ = 102.28 (3)°, and $\gamma$ = 84.27 (3)°. Three-dimensional anisotropic least-squares refinement of all atoms resulted in final discrepancy factors of $R_1(F)$ = 3.6% and $R_2(F)$ = 4.4% for 906 observed independent reflections with $I > 2\sigma(I)$. The $Fe_2(CO)_6(\mu\text{-}Se_2)$ molecule possesses an idealized $C_{2v}$-$2mm$ geometry with an Fe–Fe bond distance of 2.575 (2) Å, a Se–Se bond distance of 2.293 (2) Å, and an average Fe–Se bond distance of 2.364 Å.

## Introduction

The dinuclear iron carbonyl disulfide and diselenide complexes $Fe_2(CO)_6X_2$ (where X = S, Se) were first prepared and characterized by Hieber and Gruber[4] as diamagnetic solids whose infrared spectra show absorptions of only terminal carbonyl frequencies. On the basis of extensive infrared and dipole moment studies, Hieber and Beck[5] later proposed that the general molecular configuration of these complexes was of $C_{2v}$ symmetry with a nonplanar $Fe_2X_2$ fragment analogous to that of $Fe_2(CO)_6(SC_2H_5)_2$,[6] but they provided no speculation on any expected differences in the geometry and electronic configuration between the $Fe_2(CO)_6X_2$ (X = S, Se) and $Fe_2(CO)_6(SC_2H_5)_2$ complexes. A subsequent X-ray structural determination of the $Fe_2(CO)_6S_2$ molecule by Wei and Dahl[7] established that the two sulfur atoms were in fact a "sideways"-bridging disulfide ligand symmetrically coordinated to two iron tricarbonyl fragments.

Our interest in $Fe_2(CO)_6Se_2$ stemmed from our recent structural studies on the structurally and electronically related $Co_2(CO)_{6-n}[P(C_6H_5)_3]_n(\mu\text{-}X_2)$ (X = As, $n$ = 1,[8] 2;[8b] X = P, $n$ = 1[9]) complexes and from our theoretical studies on the related $Fe_2(CO)_6(\mu\text{-}X_2)$ (X = S, $NCH_3$)[10] and $Co_2(CO)_6(\mu\text{-}X_2)$ (X = P, As, $CCH_3$)[10b] complexes. This X-ray crystallographic study was carried out in order to facilitate a comparative analysis of the molecular parameters of the electronically related $Fe_2(NR)_2$, $Fe_2S_2$, and $Fe_2Se_2$ cores vs. the $Co_2(CR)_2$, $Co_2P_2$, and $Co_2As_2$ cores and to obtain precise molecular parameters required for molecular orbital calculations of the $Fe_2(CO)_6Se_2$ molecule.

## Experimental Section

**Single-Crystal Data Collection.** The compound was prepared from iron pentacarbonyl and a sodium polyselenide solution in the manner described by Hieber and Gruber.[4] Red prismatic crystals were separated from the reaction products by sublimation at 45 °C under vacuum. A suitable single crystal of approximate dimensions 0.21 mm × 0.16 mm × 0.19 mm in the [210], [010], and [0$\bar{1}$1] directions, respectively, was used for the collection of X-ray intensity data. The crystal was glued to the inner wall of an argon-filled Lindemann glass capillary with epoxy cement and mounted such that the $b$ axis was approximately parallel to the goniometer axis. The crystal was optically and then X-ray aligned on a NOVA-automated Syntex P$\bar{1}$ diffractometer equipped with a low-temperature device. The nitrogen flow rate was adjusted to maintain the temperature at −95 ± 5 °C. The angular coordinates of 15 reflections, which were carefully centered with Mo K$\alpha$ radiation ($\lambda(K\alpha_1)$ 0.709 26 Å, $\lambda(K\alpha_2)$ 0.713 54 Å), were least-squares refined to yield lattice parameters of $a$ = 7.704 (2) Å, $b$ = 11.779 (6) Å, $c$ = 6.585 (3) Å, $\alpha$ = 104.86 (4)°, $\beta$ = 102.28 (3)°, and $\gamma$ = 84.27 (3)° for a reduced triclinic unit cell of $P\bar{1}$ symmetry. The density calculated for a cell volume (at low temperature) of 563.7 (5) Å$^3$ containing two $Fe_2(CO)_6Se_2$ formula species is 2.578 g cm$^{-3}$. All atoms occupy the general twofold set of positions (2$i$): ±($x$, $y$, $z$).[11] The number of electrons in the unit cell, $F$(000), is 408.

Intensity data were collected via the $\theta$–$2\theta$ scan mode with a scintillation counter and pulse-height analyzer adjusted to admit 90% of the Mo K$\alpha$ peak. The Bragg $2\theta$ angle for the highly oriented graphite-crystal monochromator was 12.2°, while a takeoff angle of 4° was used for the incident beam. Variable scan speeds with a minimum of 4.0°/min and variable scan widths based on the overall intensity and width of the peak were employed. A (stationary crystal)–(stationary counter) background measurement for half the total scan time was made on each side of a peak. Two standard reflections were measured every 50 reflections to monitor instrument stability as well as crystal alignment and decay. No significant changes (>3%) in the intensities of these standard reflections were observed during the data collection period.

All independent reflections corresponding to the four octants $hkl$, $\bar{h}kl$, $hk\bar{l}$, and $\bar{h}k\bar{l}$, of the reciprocal lattice were collected for 3° ≤ $2\theta$ ≤ 40°. After correction of the data for background and Lorentz–polarization effects,[12a] the structure factor amplitudes were calculated[12a] and averaged.[12b] Of the 1467 reflections that were sampled, the 906 independent reflections with $I > 2\sigma(I)$ were utilized in the structural refinement. Since the transmission coefficients varied from 0.20 to 0.31, an absorption correction[12c] was applied to the data with a linear absorption coefficient, $\mu$, of 95.80 cm$^{-1}$ for Mo K$\alpha$ radiation.[13a]

**Structural Determination and Refinement.** Since $Fe_2(CO)_6(\mu\text{-}Se_2)$ and $Fe_2(CO)_6(\mu\text{-}S_2)$ have nearly identical lattice parameters, the two compounds were assumed to be isomorphous and the final coordinates for $Fe_2(CO)_6(\mu\text{-}S_2)$ were used as initial coordinates for $Fe_2(CO)_6(\mu\text{-}Se_2)$. Refinement[12d] of this model with isotropic thermal parameters gave $R_1(F)$ = 6.1% and $R_2(F)$ = 7.5%.[14] Anisotropic full-matrix least-squares refinement[12e] of all atoms reduced $R_1(F)$ to 3.6% and $R_2(F)$ to 4.4% at convergence, with no $\Delta/\sigma$ values greater than 0.1 and with a final goodness-of-fit value of 1.28. The minimum data-to-parameter ratio throughout the refinement was 6:1. A final Fourier difference map[12f] showed no unusual features, with the largest peak maximum being only 1.3 e/Å$^3$. Real and imaginary corrections to the atomic scattering factors[15] due to anomalous dispersion were applied for iron ($\Delta f'$ = −0.1, $\Delta f''$ = 2.4) and selenium ($\Delta f'$ = 0.4, $\Delta f''$ = 1.0).[13b]

The positional and thermal parameters from the output of the final full-matric least-squares cycle are given in Table I. Interatomic distances and bond angles with standard deviations, calculated with the Busing–Martin–Levy ORFFE program,[12g] are given in Table II. Selected least-squares planes[12h] are given in Table III. The observed and calculated structure factors are available as supplementary material.

## Results and Discussion

Crystalline $Fe_2(CO)_6Se_2$ consists of discrete dimeric molecules of the configuration shown in Figures 1 and 2. As expected, the overall molecular geometry of $Fe_2(CO)_6Se_2$ is analogous to that of $Fe_2(CO)_6(\mu\text{-}S_2)$.[7] Although no crystallographic constraints are imposed upon the molecular geometry, the configuration is nearly one of $C_{2v}$-$2mm$ sym-

0020-1669/79/1318-3060$01.00/0 

Table I. Atomic Positional (×1) and Thermal (×10[4]) Parameters[a] for $Fe_2(CO)_6(\mu\text{-}Se_2)$

| | $x$ | $y$ | $z$ | $\beta_{11}$[b] | $\beta_{22}$ | $\beta_{33}$ | $\beta_{12}$ | $\beta_{13}$ | $\beta_{23}$ |
|---|---|---|---|---|---|---|---|---|---|
| Fe(1) | 0.4939 (2) | 0.2724 (1) | 0.6354 (2) | 81 (3) | 38 (1) | 133 (5) | 8 (2) | 21 (3) | 32 (2) |
| Fe(2) | 0.8233 (2) | 0.2310 (1) | 0.7910 (2) | 75 (3) | 37 (3) | 133 (5) | 2 (2) | 20 (3) | 12 (2) |
| Se(1) | 0.6283 (1) | 0.3533 (1) | 0.9934 (2) | 120 (3) | 37 (1) | 147 (4) | 8 (1) | 39 (2) | 5 (1) |
| Se(2) | 0.7119 (2) | 0.4160 (1) | 0.7278 (2) | 139 (3) | 37 (1) | 255 (4) | −6 (1) | 57 (3) | 40 (2) |
| C(1) | 0.2888 (17) | 0.3571 (10) | 0.5994 (18) | 139 (29) | 40 (11) | 189 (37) | −2 (15) | 71 (26) | 38 (16) |
| O(1) | 0.1531 (12) | 0.4081 (8) | 0.5704 (14) | 130 (19) | 81 (9) | 321 (31) | 43 (11) | 50 (19) | 71 (13) |
| C(2) | 0.4062 (13) | 0.1452 (10) | 0.6640 (15) | 72 (23) | 48 (11) | 83 (31) | 11 (13) | −10 (21) | 17 (15) |
| O(2) | 0.3445 (11) | 0.0655 (7) | 0.6804 (12) | 177 (19) | 51 (8) | 224 (26) | −20 (10) | 1 (18) | 42 (12) |
| C(3) | 0.5130 (14) | 0.2089 (10) | 0.3633 (21) | 101 (24) | 46 (11) | 204 (42) | 3 (12) | 13 (25) | 54 (18) |
| O(3) | 0.5284 (10) | 0.1677 (7) | 0.1896 (13) | 140 (17) | 84 (9) | 148 (26) | 8 (9) | 53 (17) | 51 (12) |
| C(4) | 1.0377 (18) | 0.2661 (10) | 0.9654 (19) | 165 (30) | 39 (11) | 191 (38) | −1 (14) | 50 (30) | 26 (16) |
| O(4) | 1.1718 (11) | 0.2871 (8) | 1.0713 (14) | 89 (18) | 118 (11) | 279 (31) | −17 (11) | −69 (20) | 23 (14) |
| C(5) | 0.7982 (13) | 0.0924 (11) | 0.8470 (17) | 70 (23) | 45 (11) | 142 (34) | 8 (13) | 23 (21) | −8 (16) |
| O(5) | 0.7814 (10) | 0.0045 (7) | 0.8773 (13) | 144 (18) | 41 (8) | 273 (28) | 7 (9) | 58 (17) | 41 (12) |
| C(6) | 0.8994 (14) | 0.1694 (10) | 0.5473 (19) | 82 (23) | 61 (12) | 126 (35) | 9 (13) | 18 (24) | 34 (17) |
| O(6) | 0.9525 (10) | 0.1315 (8) | 0.3936 (14) | 136 (18) | 103 (10) | 184 (27) | 0 (10) | 62 (19) | 12 (13) |

[a] The standard deviation of the last significant figure is given in parentheses after the number. [b] The anisotropic temperature factors are of the form $\exp[-(h^2\beta_{11} + k^2\beta_{22} + l^2\beta_{33} + 2hk\beta_{12} + 2hl\beta_{13} + 2kl\beta_{23})]$.

Table II. Distances and Angles[a] for $Fe_2(CO)_6(\mu\text{-}Se_2)$

A. Bonding Distances (Å)

| | | | |
|---|---|---|---|
| Fe(1)-Fe(2) | 2.575 (2) | Fe(1)-Se(1) | 2.354 (2) |
| Se(1)-Se(2) | 2.293 (2) | Fe(1)-Se(2) | 2.378 (2) |
| | | Fe(2)-Se(1) | 2.355 (2) |
| | | Fe(2)-Se(2) | 2.366 (2) |
| | | av | 2.364 |
| Fe(1)-C(1) | 1.79 (1) | C(1)-O(1) | 1.16 (1) |
| Fe(1)-C(2) | 1.77 (1) | C(2)-O(2) | 1.13 (1) |
| Fe(1)-C(3) | 1.79 (1) | C(3)-O(3) | 1.15 (1) |
| Fe(2)-C(4) | 1.82 (1) | C(4)-O(4) | 1.13 (1) |
| Fe(2)-C(5) | 1.80 (1) | C(5)-O(5) | 1.14 (1) |
| Fe(2)-C(5) | 1.78 (1) | C(6)-O(6) | 1.13 (1) |
| av | 1.79 | av | 1.16 |

B. Bond Angles (deg)

| | | | |
|---|---|---|---|
| Fe(1)-Se(1)-Fe(2) | 66.3 (1) | Se(1)-Fe(1)-Se(2) | 58.0 (1) |
| Fe(1)-Se(2)-Fe(2) | 65.8 (1) | Se(1)-Fe(2)-Se(2) | 58.1 (1) |
| av | 66.1 | av | 58.1 |
| Fe(1)-Se(2)-Se(1) | 56.8 (1) | Se(1)-Se(2)-Fe(1) | 60.5 (1) |
| Fe(1)-Fe(2)-Se(2) | 57.3 (1) | Se(1)-Se(2)-Fe(2) | 60.7 (1) |
| Fe(2)-Fe(1)-Se(1) | 56.9 (1) | Se(2)-Se(1)-Fe(1) | 61.5 (1) |
| Fe(2)-Fe(1)-Se(2) | 56.9 (1) | Se(2)-Se(1)-Fe(2) | 61.2 (1) |
| av | 57.1 | av | 61.0 |
| Fe(1)-C(1)-O(1) | 177 (1) | Fe(2)-C(4)-O(4) | 179 (1) |
| Fe(1)-C(2)-O(2) | 178 (1) | Fe(2)-C(5)-O(5) | 178 (1) |
| Fe(1)-C(3)-O(3) | 179 (1) | Fe(2)-C(6)-O(6) | 178 (1) |

[a] The standard deviation of the last significant figure is given in parentheses after the number.

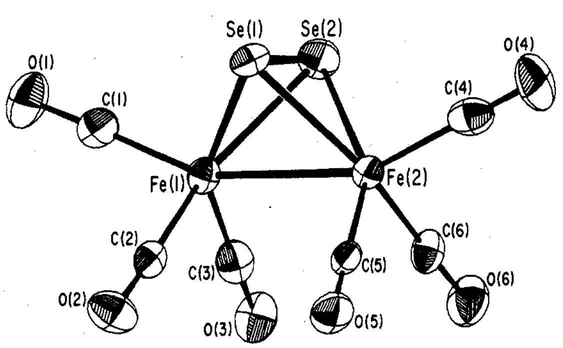


Figure 1. Configuration of the $Fe_2(CO)_6(\mu\text{-}Se_2)$ molecule showing the atom-labeling scheme. All atoms are represented by 50% thermal ellipsoids.

metry. This molecular symmetry is clearly illustrated in Figure 2, which presents a view down the pseudo-twofold axis defined by the Fe–Fe and Se–Se midpoints. The intermolecular distances, which are all greater than 3.0 Å, are similar to those found in $Fe_2(CO)_6(\mu\text{-}S_2)$ and suggest that van der Waals forces are primarily responsible for the interactions between molecules.

Table III. Distances (Å) of Atoms from Selected Least-Squares Planes[a] in the $Fe_2(CO)_6(\mu\text{-}Se_2)$ Molecule and Angles (deg) between the Normals of These Planes

A. Distances from the Plane Formed by Se(1), Se(2), C(2), and C(3)

$$-0.757X + 0.648Y - 0.084Z + 1.736 = 0$$

| | | | | | |
|---|---|---|---|---|---|
| Se(1) | −0.03 | C(3) | −0.03 | O(3) | −0.31 |
| Se(2) | 0.03 | Fe(1) | 0.38 | C(1) | 2.16 |
| C(2) | 0.03 | O(2) | −0.15 | O(1) | 3.31 |

B. Distances from the Plane Formed by Se(1), Se(2), C(5), and C(6)

$$-0.772X - 0.138Y - 0.620Z + 7.175 = 0$$

| | | | | | |
|---|---|---|---|---|---|
| Se(1) | −0.01 | C(6) | −0.01 | O(6) | −0.16 |
| Se(2) | 0.01 | Fe(2) | −0.34 | C(4) | 2.16 |
| C(5) | 0.01 | O(5) | −0.01 | O(4) | −3.28 |

C. Distances from the Plane Formed by Fe(1), Fe(2), and the Midpoint of Se(1)–Se(2)

$$0.471X + 0.490Y - 0.732Z + 0.292 = 0$$

| | | | | | |
|---|---|---|---|---|---|
| Se(1) | −1.15 | O(2) | −2.12 | C(5) | −1.30 |
| Se(2) | 1.15 | C(3) | 1.30 | O(5) | −2.10 |
| C(1) | 0.01 | O(3) | 2.13 | C(6) | 1.35 |
| O(1) | 0.01 | C(4) | −0.05 | O(6) | 2.22 |
| C(2) | −1.29 | O(4) | −0.06 | | |

D. Distances from the Plane Formed by Se(1), Se(2), and the Midpoint of Fe(1)–Fe(2)

$$-0.880X + 0.288Y - 0.379Z + 5.003 = 0$$

| | | | | | |
|---|---|---|---|---|---|
| Fe(1) | 1.29 | O(2) | 1.75 | C(5) | −1.53 |
| Fe(2) | −1.29 | C(3) | 1.44 | O(5) | −1.67 |
| C(1) | 2.93 | O(3) | 1.51 | C(6) | −1.56 |
| O(1) | 4.02 | C(4) | −2.93 | O(6) | −1.76 |
| C(2) | 1.54 | O(4) | −3.96 | | |

E. Angles between Normals to the Planes

| | | | |
|---|---|---|---|
| A and B | 56.8 | B and C | 88.7 |
| A and C | 88.6 | B and D | 29.0 |
| A and D | 27.9 | C and D | 89.7 |

[a] The equations of the planes are given in an orthogonal angstrom coordinate system ($X$, $Y$, $Z$) which is related to the fractional triclinic unit cell coordinate system ($x$, $y$, $z$) as follows: $X = xa + yb + zc \cos\beta$, $Y = yb + zc \cos\mu$, $Z = zc \sin\sigma$. In the transformations $\cos\mu = (\cos\alpha - \cos\beta\cos\gamma)/\sin\gamma$ and $\sin\sigma = (1 - \cos^2\beta - \cos^2\mu)^{1/2}$.

In the $Fe_2(CO)_6(\mu\text{-}Se_2)$ molecule, each iron atom is coordinated to two selenium atoms and to three carbonyl ligands such that the five ligands are located at the corners of a distorted tetragonal pyramid. The degree of distortion of the five ligands about each iron atom from a regular tetragonal pyramid is revealed by a calculation of the "best" basal plane

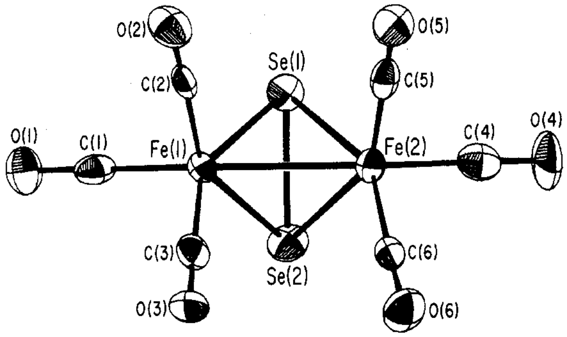


**Figure 2.** View of the $Fe_2(CO)_6(\mu\text{-}Se_2)$ molecule illustrating the idealized $C_{2v}$ molecular symmetry. All atoms are represented by 50% thermal ellipsoids.

**Table IV.** Comparison of Molecular Bond Lengths (Å) and Bond Angles (deg) of $Fe_2(CO)_6(\mu\text{-}X_2)$, Where X = S or Se

| | X = S | X = Se |
|---|---|---|
| Fe–Fe | 2.552 (2) | 2.575 (2) |
| Fe–X | 2.228 (2)[a] | 2.364 (2)[a] |
| X–X | 2.007 (5) | 2.293 (2) |
| Fe–C | 1.776 (5)[a] | 1.79 (1)[a] |
| C–O | 1.42 (6)[a] | 1.16 (1)[a] |
| Fe–X–Fe | 69.9 (1)[a] | 66.1 (1)[a] |
| X–Fe–X | 53.5 (1)[a] | 58.1 (1)[a] |
| *b* | 79.8 (1) | 77.1 (1) |

[a] The average value of the esd denotes the arithmetic mean of the individual esd's of the equivalent bond distances or angles. [b] Dihedral angle formed between two planes, each defined by the two bridge atoms and one iron atom.

(comprised of the two selenium atoms and the two equatorial carbonyl ligands) as given in Table IIIA and IIIB. The iron atoms are displaced by 0.38 and 0.34 Å from their respective basal planes in the directions toward their apical carbonyl ligands compared to corresponding displacements of 0.32 and 0.34 Å for $Fe_2(CO)_6(\mu\text{-}S_2)$. The dimeric $Fe_2(CO)_6(\mu\text{-}Se_2)$ molecule may then be described as arising from the intersection of the basal planes of the two distorted tetragonal pyramids along the Se–Se bond at a sharp dihedral angle of 56.8° (compared to 59.7° for $Fe_2(CO)_6(\mu\text{-}S_2)$). The resulting six-coordination about each iron atom can be viewed conceptually as octahedral-like with a bent Fe–Fe bond occupying the sixth coordination site.

The *idealized* $C_{2v}$ molecular geometry is evidenced by the two molecular symmetry planes (Table IIIE, and D) which are approximately perpendicular to each other (dihedral angle 89.7°). One plane is defined by atoms Fe(1), Fe(2), and the midpoint of Se(1) and Se(2), while the other plane passes through Se(1), Se(2), and the midpoint of Fe(1) and Fe(2). Examination of the perpendicular distances of the pairs of equivalent atoms from these symmetry planes establishes the corresponding atoms to be essentially equidistant on opposite sides of these approximate mirror planes. A pseudo-twofold axis in the third direction is generated from the line of intersection of the two mirror planes.

The resemblance of the molecular configurations of $Fe_2(CO)_6(\mu\text{-}Se_2)$ and $Fe_2(CO)_6(\mu\text{-}S_2)$ is depicted in Figure 3, and a comparison of their molecular parameters is summarized in Table IV. The most notable feature of the comparison of these two structures is the remarkable similarity in all comparable bond lengths and bond angles. The average of the four equivalent Fe–Se bond lengths in $Fe_2(CO)_6(\mu\text{-}Se_2)$ is 0.15 Å longer than the average Fe–S bond length in $Fe_2(CO)_6(\mu\text{-}S_2)$, while the Se–Se distance is 0.29 Å longer than the corresponding S–S distance. These changes in the Fe–X and X–X distances as a sulfur atom is replaced by a selenium

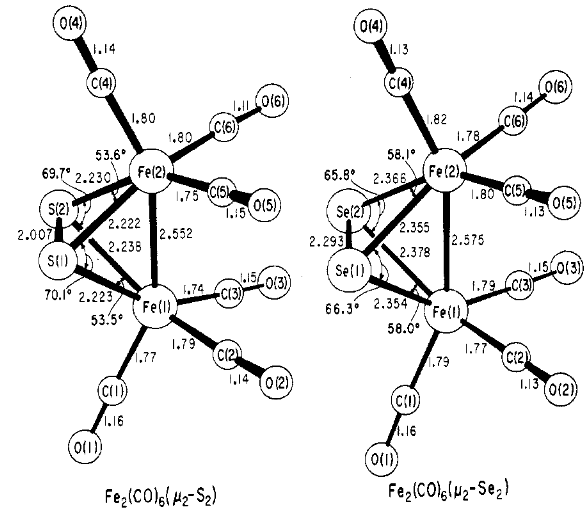


**Figure 3.** Comparison of the molecular geometries of $Fe_2(CO)_6(\mu\text{-}S_2)$ and $Fe_2(CO)_6(\mu\text{-}Se_2)$.

atom correlate well with the 0.13-Å difference in the covalent radii for sulfur (1.04 Å) and selenium (1.17 Å).[16] Similar differences in Fe–X bond lengths were observed for the $Fe_3(CO)_9(\mu_3\text{-}X)_2$ (where X = S,[17] Se[18]) complexes which exhibited average Fe–S and Fe–Se distances of 2.23 and 2.35 Å, respectively. The observed Se–Se distance of 2.293 (2) Å in $Fe_2(CO)_6(\mu\text{-}Se_2)$ is significantly shorter than the normal Se–Se single-bond distances of 2.33 (1) to 2.38 (1) Å[19] but is considerably longer than the Se–Se double-bond distance of 2.152 (3) Å found in $Se_2$.[20] This Se–Se distance in $Fe_2(CO)_6(\mu\text{-}Se_2)$ corresponds to an estimated Se–Se valence bond order of ca. 1.4. The Fe–Fe separation of 2.575 (2) Å in the selenium-bridged diiron hexacarbonyl dimer is nearly identical with that of 2.552 (2) Å observed in the corresponding sulfur-bridged dimer. The fact that the Fe–Se bond lengths are ca. 0.15 Å longer than the Fe–S bond lengths is consistent with the Fe–Se–Fe angle of 66.1 (1)° being significantly more acute than the Fe–S–Fe angle of 69.9 (1)°.

Although all Fe–C and C–O bond distances possess relatively low individual standard deviations (see Table II), no significant differences are observed between the apical and basal carbonyl bond lengths. The average Fe–C and C–O bond lengths of 1.79 (1) and 1.16 (1) Å, respectively, for $Fe_2(CO)_6(\mu\text{-}Se_2)$ are reasonably close to the mean Fe–C and C–O distances of 1.776 (5) and 1.142 (6) Å, respectively, found for $Fe_2(CO)_6(\mu\text{-}S_2)$. All six Fe–C–O bond angles are within 3° of being linear.

The important structural parameters for seven $M_2(\mu\text{-}X_2)$-type dinuclear metal cluster complexes possessing an $M_2X_2$ core with an X–X bond are summarized in Table V. The $M_2X_2$ cores as well as the unsubstituted $M_2(CO)_6(\mu\text{-}X_2)$ molecules conform to an idealized $C_{2v}$-$2mm$ geometry. The triphenylphosphine derivatives are all substituted at axial positions (trans to the metal–metal bond).

The differences among the corresponding parameters of these dinuclear metal complexes can be attributed largely to size effects arising from the different covalent radii of the bridging X atoms, as is quite evident from the M–X distances. Table VI contains estimated covalent radii for the iron and cobalt atoms which were obtained from the determined M–X distances by subtraction of the presumed single-bond radii of the bridging atoms. One point that emerges from this comparison is that the covalent radius for a given metal atom in these complexes remains relatively constant as the bridging ligand is changed, with the calculated cobalt radii (1.16–1.18 Å) being slightly smaller than the corresponding iron radii (1.18–1.19 Å). These results indicate that the metal–ligand

**Table V.** Mean Geometrical Parameters for $M_2(CO)_{6-n}[P(C_6H_5)_3]_n(\mu\text{-}X_2)$ Complexes

| compd | M | X | *n* | M-M, Å | M-E,[a] Å | E-E, Å | E-M-E, deg | M-E-M, deg | *b*, deg | *c*, deg | ref |
|---|---|---|---|---|---|---|---|---|---|---|---|
| I | Fe | $NCH_3$ | 0 | 2.496 (3) | 1.878 (3) | 1.366 (8) | 42.7 (2) | 83.0 (2) | 91.1 (2) | 68.7 (2) | 21 |
| II | Fe | S | 0 | 2.552 (2) | 2.228 (5) | 2.007 (2) | 53.6 (1) | 69.9 (1) | 79.8 (1) | 59.7 (1) | 7 |
| III | Fe | Se | 0 | 2.575 (2) | 2.364 (2) | 2.293 (2) | 58.0 (1) | 66.0 (1) | 77.1 (1) | 56.8 (1) | this work |
| IVa | Co | $CC_6H_5$ | 0 | 2.48 | 1.94 | 1.37 | 44 | 78 | 87 | 66 | 22 |
| Va | Co | P | 1 | 2.574 (3) | 2.264 (5) | 2.019 (9) | 53.0 (2) | 69.4 (2) | 79.0 (2) | 60.8 (2) | 9b |
| VIa | Co | As | 1 | 2.594 (3) | 2.386 (3) | 2.273 (3) | 56.9 (1) | 65.8 (1) | 77.7 (1) | 58.4 (1) | 8 |
| VIb | Co | As | 2 | 2.576 (3) | 2.398 (2) | 2.281 (3) | 56.8 (1) | 65.0 (1) | 78.1 (1) | 57.8 (1) | 8b |

[a] E denotes the metal-attached atom of the bridging $X_2$ ligand. [b] Dihedral angle formed between two planes, each defined by two bridge atoms and one metal atom. [c] Dihedral angle formed between two planes, each defined by two bridge atoms and the carbon atoms of two adjacent equatorial carbonyl ligands.

**Table VI.** Comparison of Calculated Covalent Radii for Metal Atoms in $M_2(CO)_{6-n}[P(C_6H_5)_3]_n(\mu\text{-}X_2)$ Complexes

| compd | M | X | *n* | M-M, Å | M-E,[a] Å | $R_E$,[b] Å | (M-E)-$R_E$, Å | ½(M-M), Å |
|---|---|---|---|---|---|---|---|---|
| I | Fe | $NCH_3$ | 0 | 2.496 | 1.878 | 0.70 | 1.18 | 1.25 |
| II | Fe | S | 0 | 2.552 | 2.228 | 1.04 | 1.19 | 1.28 |
| III | Fe | Se | 0 | 2.575 | 2.364 | 1.17 | 1.19 | 1.29 |
| IVa | Co | $CC_6H_5$ | 0 | 2.48 | 1.94 | 0.77 | 1.17 | 1.24 |
| Va | Co | P | 1 | 2.574 | 2.264 | 1.10 | 1.16 | 1.29 |
| VIa | Co | As | 1 | 2.594 | 2.386 | 1.22 | 1.17 | 1.29 |
| VIb | Co | As | 2 | 2.576 | 2.398 | 1.22 | 1.18 | 1.29 |

[a] E denotes the metal-attached atom of the bridging $X_2$ ligand. [b] Pauling's estimated single-bond covalent radii for bridging E atoms.

bonds in these complexes can be characterized by well-defined covalent radii for both metal and ligand atoms. In all cases, the metal covalent radii calculated in the above manner are significantly shorter than half the metal–metal separation. Correction of the additivity of covalent radii for electronegativity differences (or partial ionic character) would lead to slightly larger metal radii estimated from M–X bond lengths.

The considerably shorter M–M distances in the nitrogen- and carbon-bridged dimers (2.48–2.50 Å) compared to sulfur- and phosphorus-bridged dimers (2.55–2.57 Å) are primarily a consequence of the much smaller M–X distances (1.88–1.94 vs. 2.23–2.26 Å), counterbalanced to a large extent by somewhat larger M–X–M angles (78–83 vs. 67–70°). For example, with no assumed change in the angular dimensions of the $M_2X_2$-bridging system in $Fe_2(CO)_6S_2$ upon replacement of the sulfur atoms with NR groups, the Fe–Fe distance would decrease from 2.55 to only 2.04 Å (i.e., 2.55 Å × (1.88/2.26)). It is obvious that the larger Fe–N–Fe angles are primarily responsible for counterbalancing the effect on the Fe–Fe bond length of the decreased size effect of the bridging atom. An opposite effect, though much smaller in magnitude, results from the replacement of the bridging sulfur or phosphorus atoms with selenium or arsenic atoms. As a consequence of the larger M–X distances (2.36–2.40 Å) in the selenium- and arsenic-bridged dimers, the metal–metal distance increases slightly (2.58–2.59 Å) accompanied by a decrease in the M–X–M angle (65–66°). It is difficult to estimate the influence on the M–M bond strength caused by changes in the M–M distance between dimers with different X atoms due to the indivisibility of the effects of the bridging atoms on the presumed M–M single-bond interaction.

A comparison of the X–X bond lengths for these dinuclear complexes reveals nearly identical values for the $Fe_2N_2$ and $Co_2C_2$ cores (1.366 (8) vs. 1.37 Å), for the $Fe_2S_2$ and $Co_2P_2$ cores (2.007 (2) vs. 2.019 (9) Å), and for the $Fe_2Se_2$ and $Co_2As_2$ cores (2.293 (2) vs. 2.273 (3) and 2.281 (3) Å). However, an examination of these bond lengths in terms of an X–X bond order reveals an important stereochemical difference between the $Fe_2(CO)_6(\mu\text{-}X_2)$ complexes and their $Co_2(CO)_6(\mu\text{-}X_2)$ analogues. The Pauling covalent radii for homonuclear single, double, and triple bonds for nitrogen, carbon, sulfur, phosphorus, selenium, and arsenic are listed in Table VII and the corresponding (bond length)–(bond order) curves are illustrated in Figure 4. Although these

**Table VII.** Pauling Covalent Radii for Homonuclear Single, Double, and Triple Bonds

| | bond order | | |
|---|---|---|---|
| | 1 | 2 | 3 |
| N-N[a] | 1.44 | 1.24 | 1.10 |
| C-C | 1.54 | 1.34 | 1.20 |
| S-S | 2.08 | 1.88 | 1.76 |
| P-P | 2.20 | (2.00)[b] | 1.88 |
| Se-Se | 2.35 | 2.15 | (2.03)[b] |
| As-As | 2.44 | (2.24)[b] | (2.12)[b] |

[a] Homonuclear interatomic distances in angstroms. [b] The values in parentheses have been estimated from covalent radii.

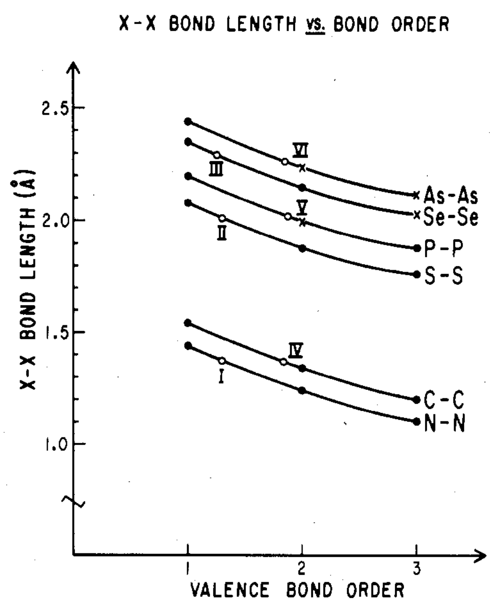


**Figure 4.** Bond length–bond order curves for X–X bonds (where X = N, C, S, P, Se, As): (●) Pauling covalent radii; (×) estimated covalent radii; (○) experimental points for $M_2(CO)_6(\mu\text{-}X_2)$ complexes. Compound designations: I, $Fe_2(CO)_6[\mu\text{-}(NR)_2]$; II, $Fe_2(CO)_6(\mu\text{-}S_2)$; III, $Fe_2(CO)_6(\mu\text{-}Se_2)$; IV, $Co_2(CO)_6[\mu\text{-}(CR)_2]$; V, $Co_2(CO)_6(\mu\text{-}P_2)$; VI, $Co_2(CO)_6(\mu\text{-}As_2)$.

(bond length)–(bond order) curves are only approximate, they demonstrate that equal bond lengths may correspond to considerably different valence bond orders for different elements (e.g., N vs. C, S vs. P, or Se vs. As). These curves suggest that the observed X–X bond lengths for the $M_2(CO)_6(\mu-X_2)$ complexes correspond to approximate X–X bond orders of 1.4 for the iron dimers and 1.9 for the cobalt dimers.

**Acknowledgment.** We gratefully acknowledge the financial support of these investigations by the National Science Foundation (Grant No. CHE 77-24309). The use of the UNIVAC 1110 computer at the Academic Computing Center, University of Wisconsin, Madison, was made available through partial support from the National Science Foundation and the Wisconsin Alumni Research Foundation, administered through the University Research Committee.

**Registry No.** $Fe_2(CO)_6(\mu-Se_2)$, 71341-69-0.

**Supplementary Material Available:** Observed and calculated structure factors for $Fe_2(CO)_6(\mu-Se_2)$ (7 pages). Ordering information is given on any current masthead page.

## References and Notes

(1) (a) Presented in part at the National Meeting of the American Crystallographic Association, Norman, OK, March 1978. (b) Based in part upon a dissertation submitted by C.F.C. to the Graduate School of the University of Wisconsin, Madison, in partial fulfillment of the requirements for the Ph.D. degree, December 1975.
(2) Department of Chemistry, University of New Mexico, Albuquerque, NM 87131.
(3) To whom correspondence should be addressed.
(4) Hieber, W.; Gruber, J. *J. Anorg. Allg. Chem.* **1958**, *296*, 91–8.
(5) Hieber, W.; Beck, W. *Z. Anorg. Chem.* **1969**, *305*, 265–70.
(6) Wei, C. H.; Dahl, L. F. *Inorg. Chem.* **1963**, *2*, 328–33.
(7) Wei, C. H.; Dahl, L. F. *Inorg. Chem.* **1965**, *4*, 1–11.
(8) (a) Foust, A. S.; Foster, M. S.; Dahl, L. F. *J. Am. Chem. Soc.* **1969**, *91*, 5633–5. (b) Foust, A. S.; Campana, C. F.; Sinclair, J. D.; Dahl, L. F. *Inorg. Chem.*, companion paper in this issue.
(9) (a) Vizi-Orosz, A.; Palyi, G.; Markó, L. *J. Organomet. Chem.* **1973**, *60*, 625–6. (b) Campana, C. F.; Vizi-Orosz, A.; Palyi, G.; Markó, L.; Dahl, L. F. *Inorg. Chem.*, preceding paper in this issue.
(10) Teo, B. K.; Hall, M. B.; Fenske, R. F.; Dahl, L. F. *Inorg. Chem.* **1975**, *14*, 3103–17. (b) Campana, C. F.; Dahl, L. F., unpublished results.
(11) "International Tables for X-Ray Crystallography"; Kynoch Press: Birmingham, England, 1968; Vol. I, p 75.
(12) Calculations were performed on a UNIVAC 1110 computer. Programs used included original or modified versions of: (a) FOBS, a Fortran diffractometer data reduction program: Calabrese, J. F., University of Wisconsin, Madison, 1972. (b) SORTMERGE: Calabrese, J. C. Ph.D. Thesis (Appendix I), University of Wisconsin, Madison, 1971. (c) DEAR, a Fortran absorption correction program by J. F. Blount based on the method given by Busing and Levy: Busing, W. R.; Levy, H. A. *Acta Crystallogr.* **1957**, *10*, 180–2. (d) Calabrese, J. C. "A Crystallographic Variable-Matrix Least-Squares Refinement Program", University of Wisconsin, Madison, 1972. (e) Busing, W. R.; Martin, K. O.; Levy, H. A. "ORFLS, A Fortran Crystallographic Least-Squares Program", Report ORNL-TM-305; Oak Ridge National Laboratory: Oak Ridge, TN, 1962. (f) MAP, a Fortran Fourier summation and molecular assemblage program: Calabrese, J. C., University of Wisconsin, Madison, 1972. (g) Busing, W. R.; Martin, K. O.; Levy, H. A. "ORFFE, A Fortran Crystallographic Function and Error Program", Report ORNL-TM-306; Oak Ridge National Laboratory: Oak Ridge, TN, 1964. (h) PLANES: Smith, D. L. Ph.D. Thesis (Appendix IV), University of Wisconsin, Madison, 1962.
(13) (a) "International Tables for X-Ray Crystallography"; Kynoch Press: Birmingham, England, 1968; Vol. III, pp 157–62. (b) *Ibid.*, pp 215–6.
(14) $R_1 = [\sum||F_o| - |F_c||/\sum|F_o|] \times 100$ and $R_2 = [\sum w_i||F_o| - |F_c||^2/\sum w_i|F_o|^2]^{1/2} \times 100$. All least-squares refinements were based on the minimization of $\sum w_i\,||F_o| - |F_c||^2$ with the individual weights $w_i = 1/\sigma(F_o)^2$.
(15) Cromer, D. T.; Mann, J. F. *Acta Crystallogr., Sect. A* **1968**, *24*, 321–5.
(16) Pauling, L. "The Chemical Bond"; Cornell University Press: Ithaca, NY, 1967; p 136.
(17) (a) Wei, C. H.; Dahl, L. F. *Inorg. Chem.* **1965**, *4*, 493–9. (b) Huntsman, J. R. Ph.D. Thesis, University of Wisconsin, Madison, 1973.
(18) Sutton, P. W.; Dahl, L. F. *Inorg. Chem.* **1963**, *2*, 1067–9.
(19) Zingaro, R. A.; Copper, W. C. "Selenium"; Van Nostrand Reinhold: New York, 1974; p 303.
(20) (a) Davis, S. P. *Phys. Rev.* **1954**, *93*, 1959–62. (b) Maxwell, L. R.; Mosely, V. M. *Phys. Rev.* **1940**, *51*, 21–3.
(21) Doedens, R. J.; Ibers, J. A. *Inorg. Chem.* **1969**, *8*, 2709–14.
(22) (a) Sly, W. G. *J. Am. Chem. Soc.* **1959**, *81*, 18–20. (b) Brown, D. A. *J. Chem. Phys.* **1969**, *33*, 1037–43.

---

Contribution from the Department of Chemistry,
Colorado State University, Fort Collins, Colorado 80523

# Structural Variations in Macrocyclic Copper(II) Complexes. Crystal and Molecular Structure of Iodo[difluoro[3,3′-(trimethylenedinitrilo)bis(2-butanone oximato)]borato]copper(II), [Cu(cyclops)I]

OREN P. ANDERSON* and ALAN B. PACKARD

*Received May 18, 1979*

The crystal and molecular structure of [Cu(cyclops)I] (**1**, cyclops = difluoro[3,3′-(trimethylenedinitrilo)bis(2-butanone oximato)]borate) has been determined from three-dimensional single-crystal X-ray diffraction data, collected by counter techniques. The dark green crystals of **1** were monoclinic, space group $P2_1/c$ (No. 14), with four formula units in the unit cell ($a$ = 10.036 (3) Å, $b$ = 7.399 (3) Å, $c$ = 24.982 (8) Å, $\beta$ = 106.67 (1)°). The structure of **1** was refined to $R$ = 0.046 ($R_w$ = 0.047) for 1488 independent reflections with $F^2 > 3\sigma(F^2)$. The discrete, monomeric complex ions exhibited square-pyramidal coordination geometry about the central copper(II) ion, with iodide occupying the apical position and the four basal coordination sites being occupied by the nitrogen atoms of the quadridentate macrocyclic cyclops ligand. The flexible macrocyclic ligand allows a large displacement (0.38 Å) of the copper(II) ion out of the basal plane of four nitrogen atoms in the direction of the apical iodo ligand; while simultaneously maintaining strong copper(II)–nitrogen bonding (Cu–N(av) = 1.956 (7) Å). A very short, strong bond is observed between the metal atom and the apical iodo ligand (Cu–I = 2.742 (2) Å), which underscores the ability of the cyclops macrocycle to allow very strong bonds to be formed to ligands in the apical position of a square-pyramidal coordination environment about copper(II).

## Introduction

Our interest in the structures of copper(II) complexes of the macrocycle difluoro[3,3′-(trimethylenedinitrilo)bis(2-butanone oximato)]borate (**2**, hereafter referred to as cyclops) became great when the structure of the square-pyramidal cyanato-*N* adduct [Cu(cyclops)(NCO)] was found to exhibit a striking degree of metal displacement (0.58 Å) out of the basal plane of nitrogen atoms and an extremely short Cu–

 